The numerical calculations were carried out with a uniform grid for the variable v with $N_V = 32$ readings. The number of checks on the angles θ and φ was chosen, respectively, to equal $N_\theta$ and $N_\varphi$ ($\theta \in [0, \pi/2], \varphi \in [0, 2\pi]$) with a uniform interval for θ and φ. The noise level of the function $f(v, \mathbf{n})$ was taken to be equal to 1% of the maximum for $f(v, \mathbf{n})$.

Figures 1 and 2 illustrate the calculation results. The isometric results shown in Fig. 1 represent the exact distribution (4.1) in the sections $V_x = 0$ (a), $V_y = 0$ (b), and $V_z = 0$ (c). In Fig. 2 we see the corresponding sections for the reproduced distribution $F_\alpha(\mathbf{V})$ with $N_\theta = 10$, $N_\varphi = 10$.

The results of the numerical calculations demonstrate the possibility of finding a three-dimensional distribution of particles by velocity through the means of computational tomography.

## LITERATURE CITED


1. G. N. Polyakova, A. I. Ranyuk, and V. F. Erko, "Kinetic energy distribution of excited atoms arising in the dissociation of $H_2$ and $D_2$ molecules subjected to electron impact," Zh. Éksp. Teor. Fiz., 73, No. 6(12) (1977).
2. D. K. Otorbaev, V. N. Ochkin, N. G. Preobrazhenskii, et al., "Distribution of $N_2(C^3\Pi)$ molecules by velocities as they are excited in nonresonance interactions of heavy particles," Preprint, Fiz. In-t Akad. Nauk SSSR, No. 39, Moscow (1981).
3. J. L. Kinsey, "Fourier transform Doppler spectroscopy: A new means of obtaining velocity-angle distributions in scattering experiments," J. Chem. Phys., 66, No. 6 (1977).
4. Yu. E. Voskoboinikov, N. G. Preobrazhenskii, and A. I. Sedel'nikov, Mathematical Processing of Experimental Data in Molecular Gasdynamics [in Russian], Nauka, Novosibirsk (1984).
5. R. M. Luitt, "Reconstruction algorithms involving the utilization of integral transformations," TIIÉR, 71, No. 3 (1983).
6. Yu. E. Voskoboinikov, V. V. Pikalov, and A. I. Sedel'nikov, "The regularization algorithm of Fourier reconstruction," in: Abstracts, 2nd All-Union Symposium on Computational Tomography, Kuibyshev, KuAI, Kuibyshev (1985).


# A NUMERICAL AND EXPERIMENTAL STUDY OF MULTICASCADE INDUCTION ACCELERATOR OF CONDUCTORS


I. A. Vasil'ev and S. R. Petrov



UDC 621.313.17:537.856


In a number of branches of sciences and engineering it is necessary to develop high speeds for the motion of solids, and these can be achieved by placing conductors into powerful magnetic fields. An effective means of accomplishing this with high speeds is the acceleration of plane annular conductors in a pulsed magnetic field generated by a plane annular inductor [1]. However, it sometimes is necessary to accelerate three-dimensional bodies, in particular, those that are cylindrical in shape. Such conductors can be accelerated in a pulsed magnetic field generated by the inductor in the form of a solenoid coil. Multicascade accelerators of conductors can be based on the inductor system of the solenoid type, and these make it possible to achieve high velocities with limited mechanical load on the body being accelerated.

The articles in [2-4] are devoted to a theoretical study of the electromechanical processes encountered in single-cascade accelerators (containing a single acceleration coil) with a solenoid-type inductor to which power is supplied from a capacitor battery. A mathematical model of a solenoid-type inductor system has been developed in [2] involving the utilization of a method of integral equations, and where the existence of an optimum mass


Istra. Translated from Zhurnal Prikladnoi Mekhaniki i Tekhnicheskoi Fiziki, Vol. 30, No. 6, pp. 37-41, November-December, 1989. Original article submitted March 21, 1988; revision submitted July 12, 1988.

for the accelerated conductor has been established, such that the kinetic energy of the conductor may make up more than 50% of the energy initially accumulated in the capacitor battery. Using a mathematical model, in [3] we find an analysis, in approximation of circuit theory, of the influence exerted by the principal parameters of the inductor system on the electromechanical efficiency defined as the ratio of the kinetic energy of the conductor at the conclusion of the acceleration to the initial reserve of energy in the capacitor battery. It is established, in particular, that a significant increase in efficiency in a number of cases is achieved through the presence of an initial velocity for the conductor, which must lead to a relatively high efficiency in the convergence of energy in a multicascade accelerator. The authors of [4] have undertaken a numerical study of the electromagnetic processes in a solenoid-type conductor system, this study based on the method of finite differences, and it showed that the mathematical model proposed in [3] allows us, with accuracy sufficient for engineering purposes, to calculate the finite velocity of the conductor and the amplitude of the discharge current. On the other hand, the assumption of a uniform current density distribution over the axial length of the accelerated conductor prevents a detailed analysis of the conductor melting process that comes about as a result of vortex-current heating, which occurs but not identically at various parts of the conductor. Correct consideration of the Joule heating is particularly important in modeling the operation of the multicascade induction accelerator, when the accelerated conductor enters each sequential cascade, having been heated earlier in the preceding stages, with the temperature distribution and, consequently, the distribution of electrical conductivity through the volume of the conductor exhibiting a complex nature. The models developed in [2-4] can be used for a stage-by-stage design of a multicascade accelerator only in the particular case in which the inductors of the cascades are separated from each other through a sufficient distance, so that their mutual influence can be neglected.

In the general case, the theoretical model of a multicascade induction accelerator must include (Fig. 1) the conductor being accelerated, said conductor having an electrical conductivity $\gamma$ and n inductors in the form of solenoids with currents $i_1(t)$-$i_n(t)$, connected through switches $K_1$-$K_n$ to the capacitors $C_1$-$C_n$. The mathematical description of the processes in the accelerator must thus take into consideration the presence of n inductors, inductively connected to the accelerated conductor and with each other, each of which is connected to its own source of electromagnetic energy (the capacitor battery). The expression for the vector potential of the "point" circular winding with current at the point B(r, z) has the form

$$A(B, t) = \int_{S_2} K(B, E)\, j(E, t)\, dS + \sum_{k=1}^{n} \frac{i_k N_k}{S_{1,k}} \int_{S_{1,k}} K(B, G_k)\, dS,$$

where $S_2$ and $S_{1,k}$ are the cross sections of the conductor and the k-th inductor, respectively; E, G are the instantaneous integration points; K(B, E) is the kernel of the integral expression. For the point $H_k(r, z)$, belonging to the k-th inductor, we obtain

$$A(H_k, t) = \int_{S_2} K(H_k, E)\, j(E, t)\, dS + \sum_{q=1}^{n} \frac{i_q N_q}{S_{1,q}} \int_{S_{1,q}} K(H_k, G_q)\, dS$$

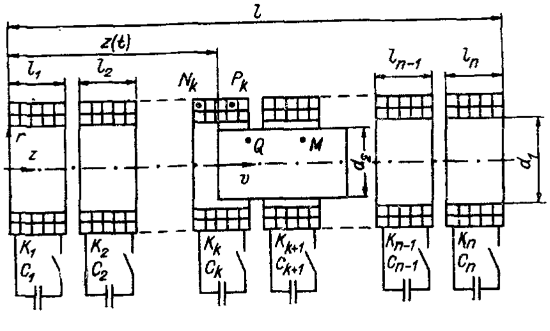


Fig. 1

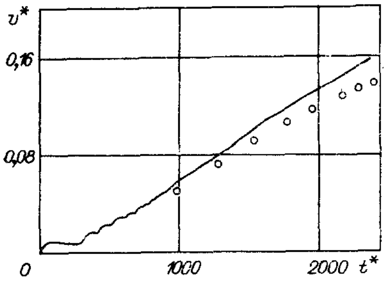


Fig. 2

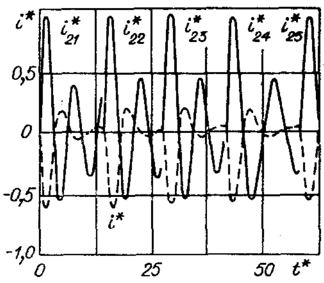


Fig. 3

($i_q$, $N_q$ is the current and the number of turns in the q-th inductor). Using the equation for the current density at point B of the conductor moving along the z axis at velocity v, we have the integrodifferential equation for the current density in the conductor:

$$\frac{j(B,t)}{\gamma(B)} + \int\limits_{S_2} K(B,E)\frac{\partial j(E,t)}{\partial t}\,dS + \sum_{k=1}^{n}\frac{N_k}{S_{1,k}}\frac{di_k}{dt}\int\limits_{S_{1,k}} K(B,G_k)\,dS + \left. + v\,\frac{i_k N_k}{S_{1,k}}\int\limits_{S1,k}\frac{\partial K(B,G_k)}{\partial z}\,dS\right] = 0.$$

For the k-th inductor we find

$$i_k(R_k + R_{0,k}) + L_{0,k}\frac{di_k}{dt} + 2\pi\frac{N_k}{S_{1,k}}\left[\int\limits_{S_{1,k}} r\,dS\int\limits_{S_2} K(G_k,E)\frac{\partial j(E,t)}{\partial t}\,dS + \right.$$

$$\left. + v\int\limits_{S_{1,k}} r\,dS\int\limits_{S_2}\frac{\partial K(G_k,E)}{\partial z}j(E,t)\,dS\right] + \frac{2\pi N_q}{S_{1,q}}\sum_{q=1}^{n}\frac{N_q}{S_{1,q}}\frac{di_q}{dt}\int\limits_{S_{1,q}} r\,dS\int\limits_{S_{1,q}} K(H_q,G)\,dS = u_k(t).$$

Here $R_k$ is the Ohmic resistance of the k-th inductors; $L_{0,k}$, $R_{0,k}$ denote the inductance and resistance of the capacitor battery, the commutator, and the connecting wires to the k-th inductor; $u_k(t)$ is the voltage at the capacitor battery of the k-th cascade; $H_q$ is the instantaneous integration point in the cross section of the q-th inductor. The equation for the discharge of the capacitor battery of the k-th cascade has the form

$$u_k(t) = -U_{0,k} - \frac{1}{C_k}\int\limits_0^t i_k\,dt$$

($C_k$ is the capacity of the battery in the k-th cascade and $U_{0,k}$ is the charge voltage). The electromagnetic force accelerating the conductor is determined from the expression

$$F = \sum_{k=1}^{n} 2\pi\frac{i_k N_k}{S_{1,k}}\int\limits_{S_2} rj(E,t)\,dS\int\limits_{S_{1,k}}\frac{\partial K(E,G_k)}{\partial z}\,dS.$$

The equations of conductor motion and for the change in electrical conductivity due to Joule heating are written as

$$m\,dv/dt = F,\ dz/dt = v,\ \partial\gamma(B)/\partial t = -j^2(B)\beta\gamma(B)/\gamma_0,$$

where m is the mass of the conductors; $\gamma_0$, $\beta$ denote the electrical conductivity of the conductor material at normal temperature and the thermal coefficient of electrical conductivity. Substituting the integrals with the finite sums according to the formula for rectangles, we obtain the following system of differential equations:

$$[L]\frac{d}{dt}[I] + v\frac{d}{dz}[L][I] + [RI] = [u].$$

Here [L] represents the matrix of the intrinsic and mutual inductions of the theoretical contours; [I] is the column of currents in the theoretical contours; [RI] is the voltage-

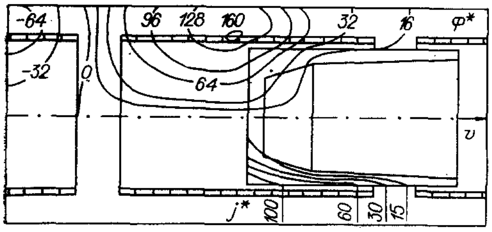


Fig. 4

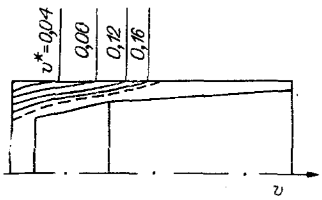


Fig. 5

drop column in the effective resistances of the contours; [u] is the column of voltages applied to the corresponding contours. In calculating the elements of the matrix [L] in accordance with [5] the theoretical contours of the conductor and the inductors of the accelerator are replaced with "thin" solenoids with a current uniformly distributed over the length. The cross section of the accelerated conductor is broken down into a uniform grid over length and radius into $n_1$ contours. The resulting system of linear algebraic equations with respect to the unknown derivatives dI/dt has a thinned-out matrix [L], many of whose elements removed from the principal diagonal are equal to zero. An effective means of solving such systems of equations involves iteration methods. The use of a simple iteration scheme brings us to the computational algorithm

$$\left(\frac{dI_i}{dt}\right)^{j+1} = \frac{1}{L_{i,i}}\left[u_i - \sum_{\substack{k=1\\k\neq i}}^{n+n_1} L_{i,k}\left(\frac{dI_k}{dt}\right)^j - v\sum_{\substack{k=1\\k\neq i}}^{n+n_1} I_k\frac{dL_{i,k}}{dz} - R_iI_i\right].$$

The system of differential equations obtained as a result of the solution for the system of algebraic equations in the Cauchy form has been solved by a Runge–Kutta method of fourth-order accuracy. In contrast to the Lavrent'ev regularization method used in [2], with an order of accuracy for the solution no higher than the second, the proposed method enables us to obtain a small truncation error and high sensitivity, which is particularly important in the modeling of relatively long processes of multicascade acceleration under conditions in which the solution, in view of the presence of a multiplicity of successively actuated switching devices, exhibits nonsmooth characteristics. Fifteen minutes were consumed on an ES-1061 computer to calculate the transient processes in a 20-cascade accelerator, with the accelerated conductor broken down into $n_1 = 8 \times 8 = 64$ contours.

An analysis of the electromagnetic processes in the device is undertaken on the example of a multicascade induction acceleration, such as we have studied experimentally. The accelerator contains 80 coaxially mounted inductors of the solenoid type, connected through air discharges to the capacitor batteries. The synchronous actuation of the discharges in conformity with the movement of the accelerated conductor was achieved by having the conductor close on the electrodes installed within the channel of the accelerator. Selecting as our basis quantities the values

$$L_* = L'd_1,\quad C_* = C'd_1,\quad U_* = \frac{1}{n}\sum_{k=1}^{n} U_{0,k},\quad x_* = d_1,$$

where L', C' are the averaged linear (per unit length of accelerator) inductance of the winding and the capacitance:

$$L' = \pi\mu_0(d_1N')^2/4,\quad C' = \sum_{k=1}^{n} C_k/l,\quad N' = \sum_{k=1}^{n} N_k/l,$$

we obtain a set of dimensionless quantities which determine the parameters of the k-th cascade:

$$d^* = d_2/x_*,\quad L_k^* = L_{0,k}/L_*,\quad C_k^* = C_k/C_*,$$
$$U_k^* = U_{0,k}/U_*,\quad R_k^* = R_{0,k}\sqrt{C_*/L_*},\quad l_k^* = l_k/x_*,$$
$$v^* = v\sqrt{C_*L_*}/x_*,\quad m^* = mx_*^2/(C_*U_*)^2L_*.$$

In the case under consideration we have $C_1^*-C_{80}^* = 2.3$, $U_1^*-U_{80}^* = 1.0$, $L_1^*-L_{80}^* = 0.3$, $R_1^*-R_{80}^* = 0.045$, $N_1-N_{10} = 14$, $N_{11}-N_{40} = 9$, $N_{41}-N_{80} = 4$, $d^* = 0.91$, $m^* = 1250$, $\ell_1^*-\ell_{80}^* = 1.76$.

Figure 2 shows the theoretical relationship between the relative velocity $v^*$ of the conductor and the time $t^* = t/\sqrt{L_* C_*}$, as well as the experimental points. The divergence between the theoretical and experimental values for the velocity of the conductor on cessation of the acceleration amounted to 15% and is basically explained by the fact that no provision was made in the mathematical model for the resistance of the air. The total efficiency of the accelerator amounted to 17.4% in calculation and to 14.3% in the experiment, while the efficiencies of the individual cascades varied in limits of 13-24% and 11-20%, respectively. Fragments of the theoretical curves for the discharge currents in the 21st through 25th cascades ($i_{21}^*-i_{25}^*$) and the total current flowing in the conductor ($i^*$) can be seen in Fig. 3, where $i_k^* = i_k/i_*$, $i_* = U_*\sqrt{C_*/L_*}$.

Figure 4 shows the theoretical distribution of the current density $j^* = j/j_*$ through the cross section of the conductor as well as the theoretical distribution of the magnetic flux $\Phi^* = \Phi/\Phi_*$ in the accelerator channel. Here $j_* = i_*/x_*^2$, $\Phi_* = \mu_0 i_*/x_*^3$, with the curves corresponding to the maximum discharge current in the 10th cascade. Figure 5 shows the theoretical and experimental curves corresponding to the melting points of the conductor for various velocities $v^*$, while the dashed line represents the limit at which the conductor melts at the end of the acceleration, a value derived experimentally. According to the calculations, when the number of cascades is increased above 80 the limit velocity corresponding to the destruction of the conductor as a result of melting would amount to $v^* \simeq 0.18$. Thus, experimentally we reached an acceleration velocity amounting to 78% of the maximum velocity in terms of the melting conditions.

## LITERATURE CITED


1. V. N. Bondaletov and E. N. Ivanov, "Noncontact induction acceleration of conductors up to hypersonic velocities," Zh. Prikl. Mekh. Tekh. Fiz., No. 5 (1975).
2. V. T. Chemeris and A. D. Podol'tsev, "Investigating magnetic-pulse interactions of conducting circuits on a digital computer with consideration given to the motion of the secondary contour," Tekhn. Élektrodinamika, No. 1 (1979).
3. V. N. Bondaletov, E. N. Ivanov, S. R. Petrov, et al., "Investigating the efficiency of the acceleration of conductors in a pulsed solenoid magnetic field," Zh. Prikl. Mekh. Tekh. Fiz., No. 2 (1983).
4. G. Z. Ber, V. N. Bondaletov, and A. A. Gusarov, "Acceleration of conductors in the pulsed magnetic field of a cylindrical multiwinding inductor," Zh. Prikl. Mekh. Tekh. Fiz., No. 4 (1984).
5. P. L. Kalantarov and L. A. Tseitlin, The Theory of Induction [in Russian], Énergoatomizdat, Leningrad (1986).